Available online at www.sciencedirect.com

SciVerse ScienceDirect

Scripta Materialia 68 (2013) 241–244

Scripta MATERIALIA

www.elsevier.com/locate/scriptamat

Eliminate Kirkendall voids in solder reactions on nanotwinned copper

Tao-Chi Liu,[a] Chien-Min Liu,[a] Yi-Sa Huang,[a] Chih Chen[a,*] and King-Ning Tu[b]

[a]Department of Materials Science and Engineering, National Chiao Tung University, Hsin-chu 30010, Taiwan, Republic of China
[b]Department of Materials Science and Engineering, UCLA, Los Angeles, CA 90095, USA

Received 17 July 2012; revised 10 October 2012; accepted 17 October 2012
Available online 23 October 2012

Electroplating was used to fabricate a high density of nanotwins that exhibited the preferred (1 1 1) orientation in Cu. We found no formation of Kirkendall voids in solder reactions on the nanotwinned Cu. This was due to the high density of steps and kinks on the nanotwin boundaries, which serve as vacancy sinks. Thus the vacancy concentration cannot reach supersaturation and nucleate voids. The finding is a significant advance in the problem of solder joint reliability in microelectronic three-dimensional integrated circuit devices.
© 2012 Acta Materialia Inc. Published by Elsevier Ltd. All rights reserved.

Keywords: Kirkendall voids; Twinning; Copper; Nanostructured materials; Diffusion

When cobalt nanoparticles are annealed in sulfur or in ambient oxygen hollow particles of CoS and Co_3O_4, respectively, are obtained [1,2]. This transformation was explained by the Kirkendall effect, in which the out-diffusion flux of Co is greater than the in-diffusion flux of O_2 or S. The difference is balanced by a flux of vacancies, which condense to form a void in the center of the particle [3–5]. Although the production of hollow nanoparticles via this kinetic behavior is unique, Kirkendall voids are a well-known phenomenon occurring during inter diffusion in both bulk and thin film materials [6,7]. Because these voids are extremely undesirable in electronic products, preventing Kirkendall void formation has become a challenging issue in microelectronic technology. An example is the presence of Kirkendall voids in solder joints on Cu used in flip chip technology. Kirkendall voids significantly weaken the mechanical properties of joints such that under vibration or on impact the joint breaks. As an illustration Figure 1a and b shows cross-sectional focused ion beam (FIB) images of two solder joints before solid-state aging. There were very few or no Kirkendall voids in the interface of Cu_3Sn and Cu before aging. In Figure 1a the Cu was fabricated by conventional electrodeposition, and no nanotwins were observed in the Cu. In Figure 1b Cu was electroplated using the same electrolyte as for (1 1 1) nanotwinned Cu but at a higher current density of 120 mA cm^{-2}. After aging at 150 °C for 1000 h Kirkendall voids appeared in both joints. Figure 1c shows a large number of voids formed in Cu_3Sn for the solder joint in Figure 1a after aging. Figure 1d shows a similar image in which many Kirkendall voids were found in the solder joint shown in Figure 1b after aging. There were no densely packed nanotwins in these two samples. Therefore these two specimens served as controls. For Cu–Sn reactions Cu served as the dominant diffusion species. The Kirkendall voids may be due to unbalanced atomic flux that resulted in the super-saturation of vacancies at the interface of Cu_3Sn and Cu. In Figure 1 there were insufficient vacancy sinks in the Cu, therefore, the supersaturated vacancies nucleated and grew to form voids at the interface. In this paper we report the significant finding that when nanotwinned Cu (nt-Cu) is used in solder joints Kirkendall void formation is eliminated. In a flip chip there are thousands of solder joints, and the number will increase in the near future when through-Si-via (TSV) is used in three-dimensional (3-D) integrated circuit technology [8,9]. This finding has added importance because nt-Cu is currently being explored for application in the large-scale production of microelectronic devices.

As the trend for the miniaturization of microelectronics is approaching the limit of Moore's law the electronics industry will necessarily move from two-dimensional

* Corresponding author. Tel.: +886 3573 1814; fax: +886 3572 4727; e-mail: chih@mail.nctu.edu.tw

1359-6462/$ - see front matter © 2012 Acta Materialia Inc. Published by Elsevier Ltd. All rights reserved.
http://dx.doi.org/10.1016/j.scriptamat.2012.10.024

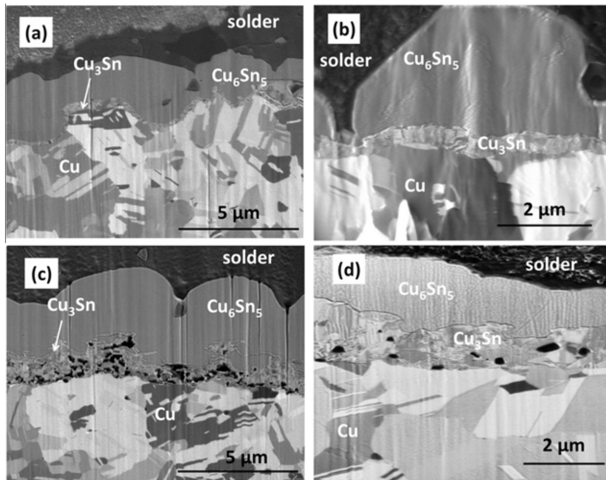

Figure 1. Cross-sectional FIB images of the Sn–Cu interface for joints with (a) polycrystalline Cu before aging, (b) the electrodeposited Cu metal layer with a random orientation before aging, (c) the polycrystalline Cu after aging at 150 °C for 1000 h and (d) the electrodeposited Cu metal layer with a random orientation after aging at 150 °C for 1000 h.

to 3-D integrated circuits, which, in essence, combine chip technology and packaging technology. The latter depends on TSV and microsolder joints. While the joint becomes smaller, the processing temperature and time remain the same, and the entire solder joint is converted to a metallic compound of Cu_6Sn_5 and Cu_3Sn by Cu–Sn reaction. The formation of Cu_3Sn is accompanied by Kirkendall voids. These voids have been a concern, and the findings described in this report provide a solution to this problem.

nt-Cu has exceptionally high mechanical strength, approximately 10 times that of ordinary Cu, but nt-Cu simultaneously maintains the same ductility and electrical conductivity [10–12], thermal stability [13], electromigration stability [14,15] and high mechanical strength [16,17] as ordinary Cu. A high density of nanotwins can be synthesized through the use of either pulsed electroplating or phase vapor deposition (PVD).

In this study we prepared nt-Cu samples by direct current (DC) electro-deposition with a $CuSO_4$ electrolyte onto a sputtered Cu seed layer on a Si wafer substrate. The [1 1 1] Cu grain orientation, as well as the [1 1 1] oriented nanotwin lamellae, were controlled by controlling the current density and stirring speed (high) of the electrolyte. Specific experimental details were described in a previous publication [18]. Next, Sn2.3Ag solder was electro-deposited on the nt-Cu layer. The samples were reflowed at 260 °C, followed by aging at 150 °C for up to 1000 h in a nitrogen-filled furnace. Interfacial microstructure examination, especially of the interface between the nt-Cu and Cu_3Sn interface, was carried out by dual beam focused ion beam (DB-FIB) and transmission electron microscopy (TEM). To avoid abrasive damage due to mechanical polishing, as well as to avoid smearing by the soft solder, which tends to obstruct void observation, all of the cross-section samples were surface polished by DB-FIB. A control sample for direct comparison was prepared under the

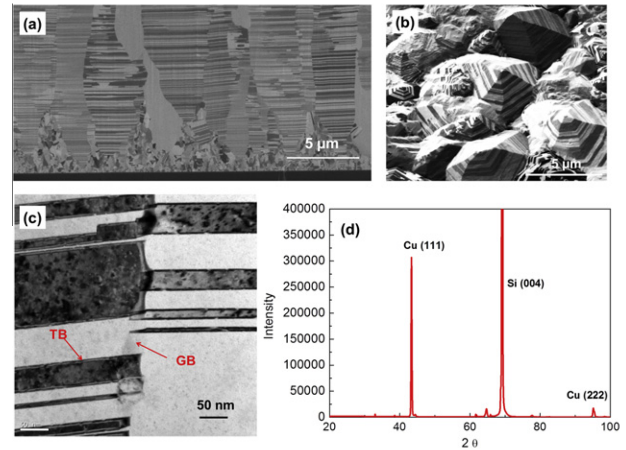

Figure 2. (a) Cross-sectional FIB image of the electrodeposited nt-Cu metal layer showing columnar grains consisting of a high density of twin lamellae. (b) Plan view of the FIB image of nt-Cu shown in (a). (c) A TEM bright field image of the grain boundaries (GB) and twin boundaries (TB) of the columnar nt-Cu. (d) X-ray diffraction for the nt-Cu metal layer. nt-Cu exhibits a strong (1 1 1) preferred orientation.

same aging conditions but using polycrystalline Cu without nanotwins, as shown in Figure 1.

It has been reported in the literature that in solid-state Sn–Cu reactions the transformation of one molecule of Cu_6Sn_5 to two molecules of Cu_3Sn releases three Sn atoms, which will attract nine Cu atoms to form three molecules of Cu_3Sn [6]. Cu dominates interdiffusion in Cu_3Sn because the sublattices have three times more Cu than Sn. The diffusion of nine Cu atoms requires the opposite diffusion of nine vacancies. If sinks cannot absorb these vacancies Kirkendall voids will form. The high density of twin planes in nt-Cu can serve as the necessary vacancy sinks.

Figure 2 shows the microstructure of nt-Cu in the as-deposited state before wetting by molten solder in reflow. Figure 2a presents a cross-sectional FIB image of the nt-Cu layer. This layer consists of columnar grains perpendicular to the Si substrate showing a high twin density, as well as highly oriented nt-Cu with the normal of the (1 1 1) twin plane parallel to the wafer surface. The grain diameter of the columnar grains varied from 0.8 to 5 µm, and the total Cu thickness was over 10 µm. Figure 2b presents a plan view FIB image of the nt-Cu surface, which exhibits a cone-like morphology. The rough surface facilitates wetting of the molten solder. Figure 2c presents a cross-sectional TEM image of the nanotwin lamellae. The thickness of nanotwin lamellae ranged from 10 to 100 nm, with an average spacing of approximately 18 nm. The two neighboring columnar grains are connected by a [1 1 1] tilt-type grain boundary, the distribution of the tilt angles being measured by electron back-scattered diffraction (EBSD). Within the distribution of tilt angles a high density of small angle tilt-type grain boundaries was found. Figure 1d shows that the [1 1 1] reflection of the columnar grains, as well as other reflections, is nearly absent, as determined by X-ray diffraction.

To observe the morphology of the Cu–Sn interface and the void distribution during solid-state reaction Fig-

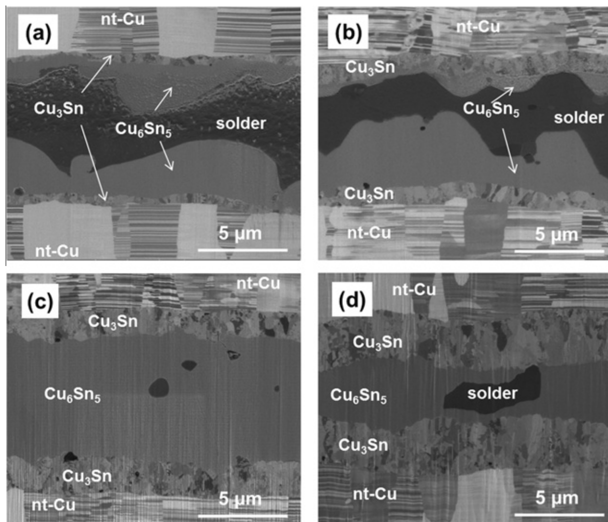

Figure 3. Cross-sectional FIB images for (a) the as-reflowed nt-Cu/Sn2.3Ag sample reflowed at 240 °C after 3 min and the solid-state sample aged at 150 °C for (b)100 h,(c) 500 h and (d) 1000 h.

ure 3a shows a cross-sectional FIB image of an as-reflowed sample. Both Cu_6Sn_5 and Cu_3Sn intermetallic compounds (IMC) are formed in the nt-Cu/Sn interface after reflow at 260 °C for 3 min. Figure 3b–d present cross-sectional FIB images after aging at 150 °C for 100, 500, and 1000 h, respectively. Both the Cu_6Sn_5 and Cu_3Sn IMCs thickened with aging time. Specifically, the Cu_3Sn IMC grew to 3.12 μm thick after aging for 1000 h, yet the entire interface contained few or no Kirkendall voids.

Cross-sectional high resolution TEM observations were employed to observe the interfacial structure of Cu_3Sn and nt-Cu. Figure 4a reveals the interfacial structure for Cu_3Sn and nt-Cu after aging for 100 h. The grain boundaries in polycrystalline Cu_3Sn formed part of the diffusion paths for Cu atoms diffusing across Cu_3Sn layer to form new Cu_3Sn at the interface. Meanwhile, vacancies also diffused to the nt-Cu side. There were several twin lamellae connected to the nt-Cu/Cu_3Sn interface. An atomic force microscope was used to measure the roughness of the nt-Cu surface. The results indicated that the average roughness (R_a) was 154 nm, which means that there were approximately

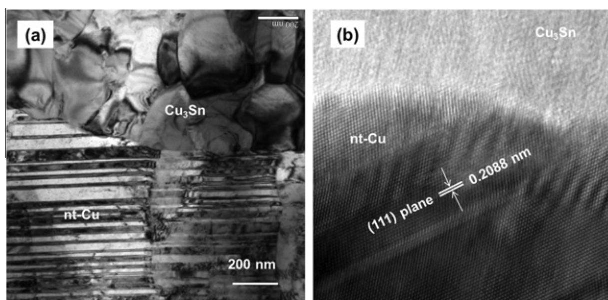

Figure 4. (a) TEM bright field image of the nt-Cu/Cu_3Sn interface after solid-state reaction for 100 h. (b) High resolution TEM of twin lamellae in contact with Cu_3Sn, showing a continuous atomic arrangement without vacancy nucleation.

15 nanotwin lamellae in contact with the solder during the initial reaction. Figure 4b presents a high resolution TEM image of the interface between the nt-Cu lamellae and Cu_3Sn. The interplanar spacing of the (1 1 1) plane in Cu was 0.2088 nm. The high resolution TEM image shows no vacancy condensation in the interface. On the (1 1 1) twinning plane there may be many steps and kinks that serve as vacancy sinks [19]. Because of the high nanotwin density the sink density is also high. Since vacancy absorption reduced the local supersaturation of vacancies no nucleation of Kirkendall voids occurred.

Kirkendall voids are often affected by impurities in the sample [20]. To eliminate the impurity effect we used the same electroplating bath to form nt-Cu, but rapidly increased the operating current density to remove nanotwin structures in the electro-deposited Cu layer. We repeated the aging experiment such that the incorporated impurities in the electroplated Cu would be the same. Figure 1b shows a cross-sectional FIB image of the interface of the Cu_3SnIMCs and the electroplated Cu film fabricated under a high current density DC. The Cu grains included no nanotwin lamellae. After solid-state aging at 150 °C for 1000 h Kirkendall voids formed in the Cu_3Sn. This result shows that once nanotwins were removed from the electro-deposited Cu film Kirkendall voids returned.

Darken's analysis of the Kirkendall effect on interdiffusion assumes an equilibrium vacancy concentration everywhere in the sample. Sources and sinks of vacancies are assumed to be fully operative; therefore the lattice shift, or Kirkendall shift, occurs as indicated by marker motion. Because there is no supersaturation of vacancies, no nucleation of voids can happen. When Kirkendall (or Frenkel) voids are found it means excess vacancies exist. Our finding of no Kirkendall void formation in nanotwinned Cu empirically supports Darken's analysis. In Darken's analysis the net difference between fluxes of A and B was balanced by the flux of vacancies. In our case this finding means that the flux difference between Cu and Sn is balanced by the vacancy flux, which, in turn, is absorbed by sinks in the nanotwinned Cu. Knowing the vacancy flux, we know the density of sinks needed. With respect to the growth of Cu_3Sn, we can assume that one-third of the Cu flux is balanced by Sn flux, and two-thirds of the Cu flux is balanced by vacancies. Therefore, if we measure the thickness of Cu_3Sn at a given time and divide the thickness by the atomic volume we know the vacancy flux.

To understand the effectiveness of vacancy sinks note that the kink on a step on a twin surface will be similar to the kink on a dislocation in climb. The kink persists because it is not able to disappear until it reaches the edge of the sample. The vacancy sinks are so effective because nanotwins have a high density of twin planes.

In summary, densely packed nanotwins in highly (1 1 1)-oriented Cu have been fabricated by DC electroplating. Oriented nt-Cu can eliminate the formation of Kirkendall voids in solder joint reactions. The nanotwin boundaries provide vacancy sinks. Therefore, the vacancy concentration cannot reach supersaturation to nucleate voids. This finding suggests a solution to the solder joint reliability problem in microelectronic devices.

The authors gratefully acknowledge financial support from the National Science Council of the Republic of China (Grant No. NSC 98-2221-E-009-036-MY3).

[1] Y.D. Yin, R.M. Rioux, C.K. Erdonmez, S. Hughes, G.A. Somorjai, A.P. Alivisatos, Science 304 (2004) 711.
[2] Y.D. Yin, C.K. Erdonmez, A. Cabot, S. Hughes, A.P. Alivisatos, Adv. Funct. Mater. 16 (2006) 1389.
[3] J.G. Railsback, A.C. Johnston-Peck, J. Wang, J.B. Tracy, ACS Nano. 4 (2010) 1913.
[4] A. Cabot, R.K. Smith, Y. Yin, H. Zheng, B.M. Reinhard, H. Liu, A.P. Alivisatos, ACS Nano. 2 (2008) 1452.
[5] Q. Peng, X.Y. Sun, J.C. Spagnola, C. Saquing, S.A. Khan, R.J. Spontak, G.N. Parsons, ACS Nano. 3 (2009) 546.
[6] K.N. Tu, Solder Joint Technology Materials, Properties, and Reliability, Springer Science, New York, 2007, pp. 58.
[7] K.N. Tu, U. Gosele, Appl. Phys. Lett. 86 (2005) 093111.
[8] R.S. Patti, Proc. IEEE 94 (6) (2006) 1214.
[9] K.N. Tu, Microelectron. Reliab. 51 (3) (2011) 517.
[10] L. Lu, Y. Shen, X. Chen, L. Qian, K. Lu, Science 304 (2004) 422.
[11] O. Anderoglu, A. Misra, F. Ronning, H. Wang, X. Zhang, J. Appl. Phys. 106 (2009) 024313.
[12] X.H. Chen, L. Lu, K. Lu, J. Appl. Phys. 102 (2007) 083708.
[13] O. Anderoglu, A. Misra, H. Wang, X.J. Zhang, Appl. Phys. 103 (2008) 094322.
[14] K.C. Chen, W.W. Wu, C.N. Liao, L.J. Chen, K.N. Tu, Science 321 (2008) 1066.
[15] K.C. Chen, W.W. Wu, C.N. Liao, L.J. Chen, K.N. Tu, J. Appl. Phys. 108 (2010) 066103.
[16] K. Lu, L. Lu, S. Suresh, Science 324 (2009) 349.
[17] L. Lu, X. Chen, X. Huang, K. Lu, Science 323 (2009) 607.
[18] H.Y. Hsiao, C.M. Liu, H.W. Lin, T.C. Liu, C.L. Lu, Y.S. Huang, C. Chen, K.N. Tu, Science 336 (2012) 1007.
[19] L. Xu, D. Xu, K.N. Tu, Y. Cai, N. Wang, P. Dixit, J.H.L. Pang, J. Miao, J. Appl. Phys. 104 (2008) 113717.
[20] J.Y. Kim, J. Yu, Appl. Phys. Lett. 92 (2008) 092109.